Histochem Cell Biol (2004) 122:539–551
DOI 10.1007/s00418-004-0714-9

ORIGINAL PAPER

Huai Zhen Ruan · Eamonn Moules · Geoffrey Burnstock

Changes in $P2X_3$ purinoceptors in sensory ganglia of the mouse during embryonic and postnatal development

Accepted: 21 September 2004 / Published online: 12 November 2004

Abstract The expression of the $P2X_3$ nucleotide receptor in embryonic day 14–18, postnatal day 1–14 and adult mouse sensory ganglia was examined using immunohistochemistry. Nearly all sensory neurons in dorsal root ganglia, trigeminal ganglia and nodose ganglia in embryos at embryonic day 14 expressed $P2X_3$ receptors, but after birth there was a gradual decline to about 50% of neurons showing positive immunostaining for $P2X_3$. In embryos there were only small neurons, while from postnatal day 7 both large and small neurons were present. Isolectin B_4 (IB_4)-positive neurons in dorsal, trigeminal and nodose ganglia did not appear until birth, but the numbers increased to about 50% by postnatal day 14 when a high proportion of IB_4-positive neurons were also positively labelled for the $P2X_3$ receptor. About 10% of neurons in dorsal, trigeminal and nodose ganglia were positive for calcitonin gene-related peptide in embryos, nearly all of which stained for $P2X_3$ receptors. This increased postnatally to about 35–40% in adults, although only a few colocalised with $P2X_3$ receptors. Neurofilament 200 was expressed in about 50% of neurons in trigeminal ganglia in the embryo, and this level persisted postnatally. All neurofilament 200-positive neurons stained for $P2X_3$ in embryonic dorsal root ganglia, trigeminal ganglia and nodose ganglia, but by adulthood this was significantly reduced. The neurons that were positive for calbindin in embryonic dorsal, trigeminal and nodose ganglia showed colocalisation with $P2X_3$ receptors, but few showed colocalisation postnatally.

H. Z. Ruan · E. Moules · G. Burnstock (✉)
Autonomic Neuroscience Institute,
Royal Free & University College Medical School,
Rowland Hill Street, London, NW3 2PF, UK
e-mail: g.burnstock@ucl.ac.uk
Tel.: +44-207-8302948
Fax: +44-207-8302949

H. Z. Ruan
Department of Neurobiology,
Third Military Medical University,
400038 Chongqing, China

Keywords Purinoceptors · $P2X_3$ receptors · ATP · Sensory ganglia · Development

Introduction

P2X receptors are a family of ligand-gated ion channels responsive to ATP. Seven subtypes have been identified which form homomultimeric or heteromultimeric pores. The $P2X_3$ receptor subunit was cloned in 1995 and shown to be predominantly localised in a subpopulation of small nociceptive sensory neurons in the dorsal root ganglia (DRG), trigeminal ganglia (TG) and nodose ganglia (NG). Subsequent immunohistochemical studies showed that these neurons were labelled with the isolectin B_4 (IB_4; Chen et al. 1995; Cook et al. 1997; Vulchanova et al. 1997, 1998; Bradbury et al. 1998; Llewellyn-Smith and Burnstock 1998; Xiang et al. 1998; Barden and Bennett 2000).

In DRG, intensive $P2X_3$ immunoreactivity is found predominantly in a subset of small- and medium-diameter neurons, which is absent from most large neurons (Vulchanova et al. 1997, 1998; Bradbury et al. 1998; Xiang et al. 1998; Novakovic et al. 1999). The $P2X_3$ subunit is present in approximately equal numbers of neurons projecting to the skin and viscera but in very few of those innervating skeletal muscle (Bradbury et al. 1998). After sciatic nerve axotomy, $P2X_3$ receptor expression decreases by about 50% in lumbar region L4/5 DRG, and this downregulation is reversed by glial cell line-derived neurotrophic factor (Bradbury et al. 1998). In contrast, after chronic constriction injury to the sciatic nerve, the number of $P2X_3$-positive small- and medium-diameter DRG neurons appeared to have increased (Novakovic et al. 1999). The reason why these different forms of nerve damage produce opposite effects of $P2X_3$ subunit expression is at present unclear. At the peripheral terminals of DRG neurons, $P2X_3$ immunoreactivity was observed in nerve fibres in rat and mouse glabrous skin, where the fibres appear to extend superficially and terminate in the epidermis (Vulchanova et al. 1998). $P2X_3$

immunoreactivity was also seen on sensory nerve terminals in the tongue (Cook et al. 1997; Bo et al. 1999; Rong et al. 2000), tooth pulp (Cook et al. 1997; Alavi et al. 2001) and on the suburothelial nerve plexus of mouse urinary bladder, with positive staining on terminals of small nerve fibres that embed in the urothelium (Cockayne et al. 2000). Following sciatic nerve ligation, $P2X_3$ immunoreactivity accumulates proximal to the ligation site, indicating that $P2X_3$ is synthesised in the cell body and transported along the processes into both central and peripheral terminals (Vulchanova et al. 1997; Novakovic et al. 1999).

In TG, $P2X_3$ receptor immunoreactivity occurs in both small and large nerve cell bodies and their processes (Cook et al. 1997; Llewellyn-Smith and Burnstock 1998; Xiang et al. 1998).

Electrophysiological studies have also been carried out to characterise $P2X_3$ receptors in recombinant receptors expressed in *Xenopus* oocytes and in sensory ganglia (Dunn et al. 2000, 2001; Liu et al. 2001; Zhong et al. 2001) and recordings made in sensory nerves following activation of terminals of these nerves in bladder (Vlaskovska et al. 2001; Rong et al. 2002). The $P2X_3$ receptor is observed mainly in capsaicin receptor vanilloid receptor subtype 1 (VR1)-positive sensory neurons (Guo et al. 1999). In capsaicin-sensitive DRG neurons, ATP and its analogue α,β-methylene ATP evoke an inward current with fast activation and inactivation (Ueno et al. 1999), which is lacking in $P2X_3$-deficient mice (Cockayne et al. 2000; Souslova et al. 2000), indicating that functional $P2X_3$ receptors are expressed in nociceptors. These results all suggest that $P2X_3$ receptor subunits may play important roles in sensory transmission.

There is growing evidence to suggest that purinergic signalling is involved in early embryonic development. Purinoceptors were shown to be one of the first functionally active membrane receptors in chick embryo cells during gastrulation, in which, by means of purinoceptors, ATP induced rapid accumulation of inositol phosphate and Ca^{2+} mobilisation in a similar way and to the same extent as acetylcholine (Laasberg 1990). Recent reports also implicate ATP as a key regulator of the development of various organs and systems in frog and chick as well as in mammalian embryos (reviewed by Burnstock 1996, 2001). $P2X_3$ receptor expression at the early stages of mouse embryogenesis has been reported, but it is interesting to note that the $P2X_3$ expression patterns were not identical in rat and mouse embryos. Mouse embryos express $P2X_3$ in many tissues (such as DRG and TG) at embryonic day 9.5 (E9.5) embryos where no corresponding expression was found in the rat (Boldogkö et al. 2002; Cheung and Burnstock 2002). Neurons in DRG began to express $P2X_3$ receptors in E12.5 rat embryos. For the TG in E11–11.5 rat embryos, $P2X_3$ was found in the neurons and fibres (Cheung and Burnstock 2002). However, we do not know the changes in numbers of sensory neurons expressing $P2X_3$ receptors during mouse embryonic and postnatal development. The relationship between $P2X_3$ receptors and other phenotypic markers has also been little studied in developing mouse. In this study, the location, quantity of $P2X_3$ receptors and relationship between $P2X_3$ receptors and other phenotypic markers including IB_4, calcitonin gene-related peptide (CGRP), neurofilament 200 (NF200) and calbindin was studied in the sensory ganglia from E14 to E18, postnatal and adult mice.

Materials and methods

Tissue preparation

The expression of $P2X_3$ receptor protein in embryonic sensory ganglia was studied in albino outbred mouse embryos of E14, E16 and E18 (five animals/stage) using immunohistochemical techniques. Postnatal mouse sensory ganglia on postnatal day 1 (P1), P7, P14 and adult (five animals/stage) were chosen for examination. The day of identification of the presence of a vaginal plug was designated as day zero (E0). Pregnant mice were killed by asphyxiation with a rising concentration of CO_2 (between 0% and 100%), and death was confirmed by cervical dislocation according to Home Office (UK) regulations covering Schedule One procedures. Embryos were collected and fixed in 4% paraformaldehyde in 0.1 M phosphate buffer (PB; pH 7.2) at 4°C, overnight. Embryos were then washed in 0.1 M phosphate-buffered saline (PBS; pH 7.2) and dehydrated using 10% sucrose, 20% sucrose and, finally, 30% sucrose. Thereafter, lumbar DRG, TG and NG were dissected and immersed in OCT-embedding medium and frozen in precooled isopropanol (–70°C) for cryosectioning. Frozen sections (10 μm) were cut and mounted on gelatin-coated slides and dried at room temperature. Postnatal mouse lumbar DRG, TG and NG were dissected after cervical dislocation and the ganglia were fixed and processed as described above. Frozen sections (10 μm) were cut and mounted.

Antisera

Rabbit anti-$P2X_3$ receptor (1:400) antibody was provided by Roche Bioscience (Palo Alto, CA, USA). The immunogens used for production of polyclonal $P2X_3$ antibody were synthetic peptides corresponding to the carboxyl terminal of the cloned rat $P2X_3$ receptors, covalently linked to keyhole limpet hemocyanin. The peptide sequences of the $P2X_3$ receptors are of amino acid sequence 383–397 (VEKQSTDSGAYSIGH). Other antibodies used are mouse anti-NF200 (clone N52; Sigma; 1:400), mouse anti-CGRP (Affiniti; 1:2,000) and mouse anti-calbindin (Swant; 1:20,000). We also used biotin-conjugated IB_4 from *Griffonia simplicifolia* (Sigma; 10 μg/ml).

Immunohistochemistry

Immunohistochemistry for P2X receptors was performed by using rabbit polyclonal antibodies against a unique peptide sequence of $P2X_3$ receptor subtypes. For immunostaining of cryosections, the standard avidin-biotin complex (ABC) technique was used. Sections were postfixed with 4% paraformaldehyde for 2 min at room temperature. Endogenous peroxidase was blocked by 0.5% H_2O_2 and 50% methanol (methanol:PBS, 1:1) for 20 min. The $P2X_3$ primary antibody was used at a concentration of 1:400, prepared in 10% normal horse serum (NHS) containing 0.2% Triton X-100, overnight. Subsequently, the sections were incubated with biotinylated donkey anti-rabbit IgG (Jackson Immunoresearch, West Grove, PA, USA) at a dilution of 1:500 in PBS containing 1% NHS for 1 h. The sections were then incubated in ExtrAvidin peroxidase diluted 1:1,000 in PBS for 1 h at room temperature. For colour reactivity, a solution containing 0.05% 3,3′-diaminobenzidine (DAB), 0.04% nickel ammonium sulphate, 0.2% β-D-glucose,

0.004% ammonium nitrate and 1.2 U/ml glucose oxidase in 0.1 M PB (pH 7.2) was applied. Sections were washed three times with 0.1 M PBS after each of the above steps (except for serum preincubation). Slides were mounted with Eukitt (BDH Laboratory, UK) and examined with light microscopy. The control experiments were carried out with the primary antibodies preadsorbed with the peptides for immunising the rabbits or the primary antibody replaced with NHS.

Following immunohistochemistry, a group of sections was counterstained with 1% neutral red. Positively and negatively immunostained neurons were counted to calculate the proportion of positive neurons. To ensure counting was unbiased, the procedure was conducted 'blind' ensuring that the operator was not aware of the developmental stage or immunostaining performed on each slide.

Immunofluorescence double labelling

In colocalisation studies investigating the coexpression of $P2X_3$ receptors and NF200, CGRP or calbindin, sections were incubated with the $P2X_3$ antibody overnight and detected with Cy3-conjugated donkey anti-rabbit IgG, incubated with either monoclonal NF200, CGRP or calbindin antibody (4°C, overnight) and detected with fluorescein isothiocyanate (FITC)-conjugated mouse antibody (raised in goat; Sigma; 1:200, 1 h). For colocalisation with IB_4, sections were immunostained for the $P2X_3$ receptor, as above, and then incubated with biotin-conjugated IB_4 (16 h) and detected with streptavidin-FITC (1:200;1 h). The sections were washed and mounted in Citifluor.

Sections on which counts of IB_4-, NF200-, CGRP- and calbindin-positive cells had been performed were marked and then counterstained with toluidine blue (2.5% in 0.1 M PB for 2 min followed by dehydration through increasing grades of alcohol, cleared in xylene and coverslipped with DPX mounting medium). This enabled the total cell profile numbers to be determined by counting all profiles in the marked sections under bright-field illumination. The percentages of total cell numbers that were IB_4-, NF200-, CGRP- and calbindin-positive were then calculated.

Photomicroscopy

Images of DAB immunochemical staining and immunofluorescence labelling were taken with the Leica DC 200 digital camera (Leica, Switzerland) attached to a Zeiss Axioplan microscope (Zeiss, Germany). Images were imported into a graphics package (Adobe Photoshop 5.0, USA). The two-channel readings for green and red fluorescence were merged by using Adobe Photoshop 5.0.

Data analysis

All analyses were performed at ×20 objective magnification. $P2X_3$ receptor, IB_4-, NF200-, CGRP- and calbindin-positive cells in ganglia were determined by counting all immunoreactive-positive cell profiles in every sixth section throughout the ganglia. Total cell profiles were counted and the percentages of total cell profiles that were $P2X_3$ receptor-, IB_4-, NF200-, CGRP- and calbindin-positive were then calculated.

To calculate percentages of $P2X_3$ receptor colocalisation with other markers, four randomly selected ganglia sections were chosen for each pair of markers, for each animal. For each section, counts were made of the number of profiles that were positive for the $P2X_3$ receptor, the number of profiles positive for the other markers (CGRP, calbindin, NF200 or IB_4) and the number of profiles expressing both antigens and percentages were calculated. All values are given as the mean ± SEM (%) and the results were statistically analysed by a one-way analysis of variance followed by a Tukey's *post hoc* test where more than five age groups were analysed. For analyses of less than five age groups, a Bonferroni's *post hoc* test was used. Although all grouping of data were compared by this test, statistical significance between each group and the one immediately preceding it has been highlighted in the tables; * $P<0.05$, ** $P<0.01$, *** $P<0.001$. For the data in Table 1, a Tukey's *post hoc* test was performed to compare embryonic days E14, E16 and E18 with postnatal ages P7, P14 and adult; *** $P<0.001$.

Results

$P2X_3$ immunoreactivity in the sensory ganglia during mouse embryonic and postnatal development

Immunohistochemistry was performed to investigate the pattern of $P2X_3$ receptor protein expression in sensory ganglia during mouse embryonic and postnatal development. Using the standard ABC method with nickel and DAB as chromogens, black staining indicated positive immunoreactivity. In this study, mouse embryos of E14, E16, E18 and postnatal P1, P7, P14 and adult mice were chosen to investigate $P2X_3$ immunoreactivity and the results are summarised in Table 1 and Fig. 1.

The intensive expression of $P2X_3$ in DRG, TG and NG persists from E14 through later stages of development and into the adult. In embryos (E14–E18), $P2X_3$ is expressed in a homogeneous pattern in almost all DRG, TG and NG neurons. By contrast, in later developmental stages (postnatal P1–P14), $P2X_3$ receptor expression is signifi-

Table 1 Expression of $P2X_3$ receptor immunoreactivity in dorsal root ganglion (*DGR*), trigeminal ganglion (*TG*), nodose ganglion (*NG*) in mouse embryonic and postnatal development. *n* Number of $P2X_3$ receptor-positive cell profiles and the total number of cell profiles counted, respectively (five animals/stage). Note statistical significance indicated by *asterisks* relates to embryonic days E14, E16 and E18, as compared with postnatal ages P7, P14 and adult

	Percentage of $P2X_3$ receptor immunopositive nerve cell bodies						
	E14	E16	E18	P1	P7	P14	Adult
DRG	100	100	97.2±1.5	92.5±2.2	72.6±3.4***	47.5±2.8***	44.3±3.5***
n	(2,053/2,053)	(2,113/2,113)	(2,026/2,087)	(1,833/1,984)	(1,404/1,937)	(897/1,891)	(816/1,838)
TG	100	100	95.4±1.8	92.2±3.2	68.6±3.6***	45.7±2.6***	43.8±2.8***
n	(2,546/2,546)	(2,467/2,467)	(2,151/2,259)	(2,074/2,248)	(1,343/1,959)	(872/1,905)	(833/1,898)
NG	100	100	97.8±2.1	96.3±1.2	88.6±3.1	65.6±3.8***	60.6±4.1***
n	(1,831/1,831)	(1,954/1,954)	(1,827/1,870)	(1,813/1,884)	(1,623/1,835)	(1,128/1,721)	(1,093/1,806)

*** $P<0.001$

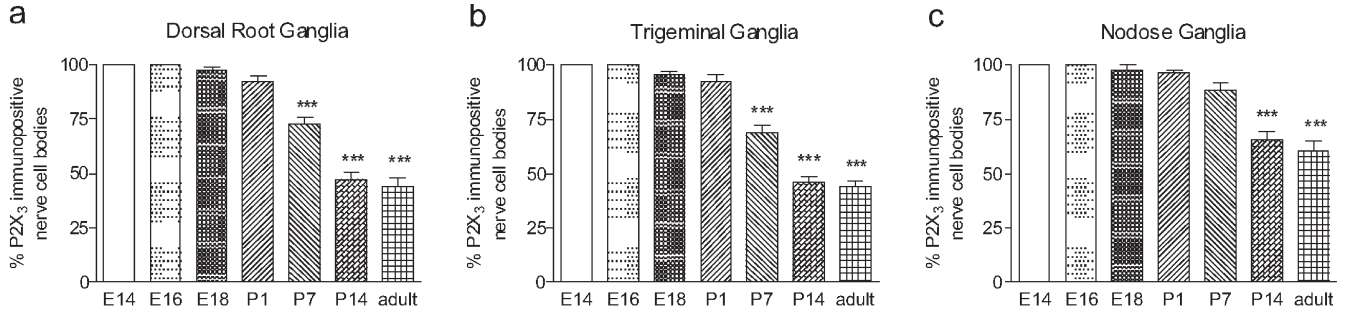

Fig. 1A–C Percentage of $P2X_3$-immunoreactive nerve cell bodies in sensory ganglia of mouse in embryonic and postnatal development. **A** Dorsal root ganglia. **B** Trigeminal ganglia. **C** Nodose ganglia. Note statistical significance indicated by *asterisks* relates to postnatal ages P7, P14 and adult as compared with embryonic days E14, E16 and E18. *** $P<0.001$

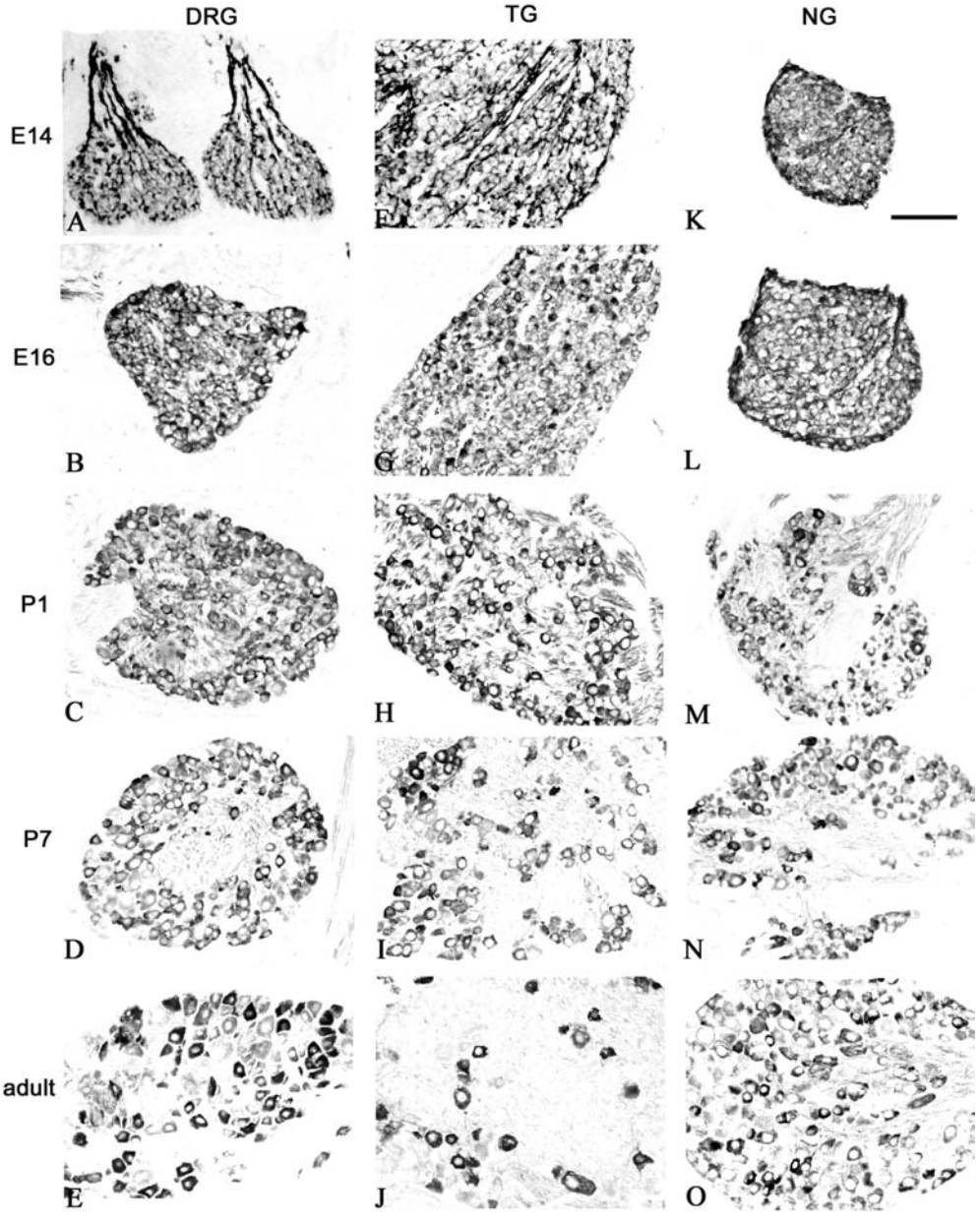

Fig. 2A–O Localisation of $P2X_3$ receptor immunoreactivity in sensory ganglia of mouse in embryonic and postnatal development. **A–E** $P2X_3$ receptor immunoreactivity in dorsal root ganglion (*DRG*). **A** E14. **B** E16. **C** P1. **D** P7. **E** Adult. **F–J** $P2X_3$ receptor immunoreactivity in trigeminal ganglion (*TG*). **F** E14. **G** E16. **H** P1. **I** P7. **J** Adult. **K–O** $P2X_3$ receptor immunoreactivity in nodose ganglion (*NG*). **K** E14. **L** E16. **M** P1. **N** P7. **O** Adult. *Scale bar* 100 μm

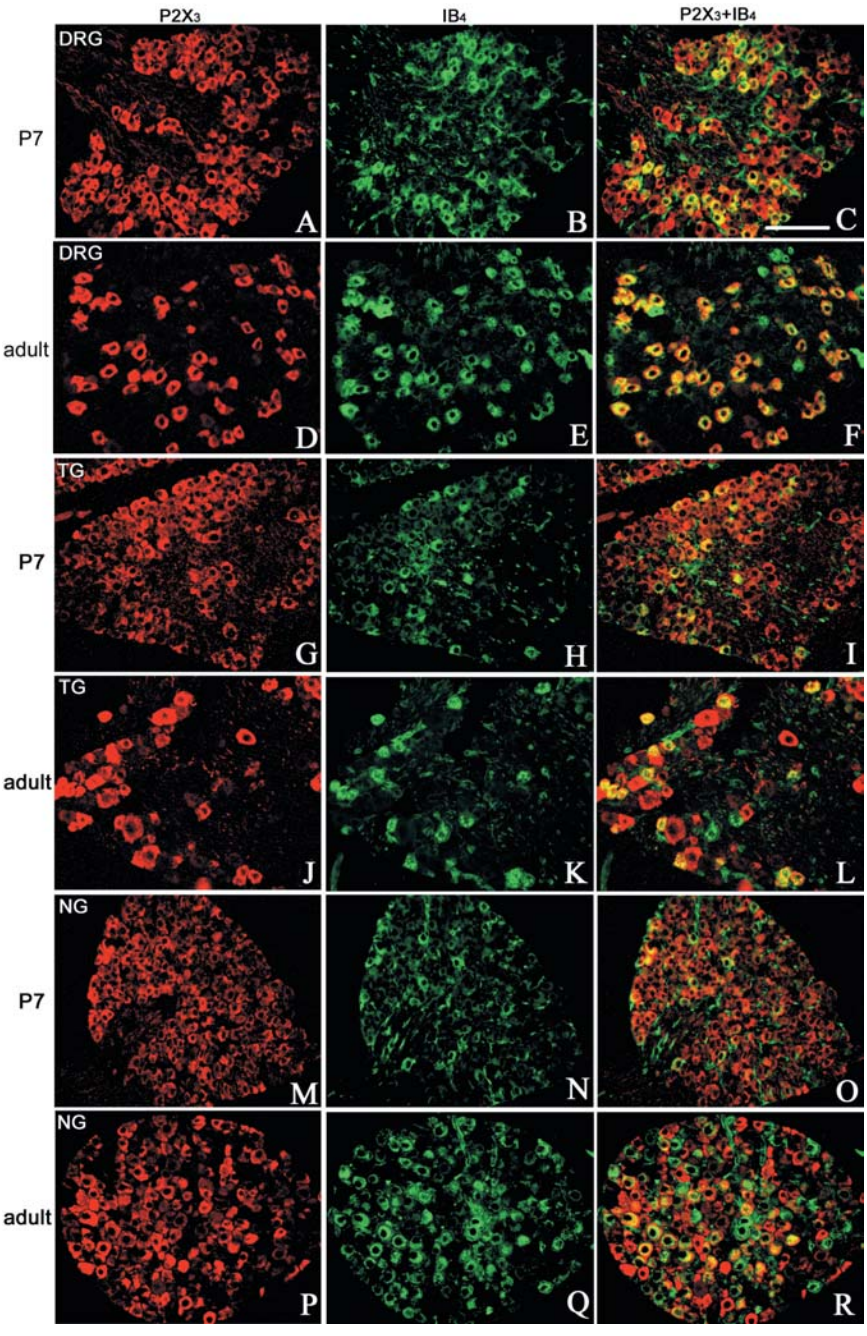

Fig. 3A–R Colocalisation (*yellow/orange*) of $P2X_3$ receptor immunoreactivity (-IR; *red*) with isolectin B_4 (*IB_4*; *green*) immunostaining in the developmental mouse sensory ganglia. **A–C** Double staining for $P2X_3$-IR and IB_4 in DRG of P7 mouse. **D–F** Double staining for $P2X_3$-IR and IB_4 in DRG of adult mouse. **G–I** Single section double stained for $P2X_3$-IR and IB_4 in TG of P7 mouse. **J–L** Double staining for $P2X_3$-IR and IB_4 in TG of adult mouse. **M–O** Double staining for $P2X_3$-IR and IB_4 in NG of P7 mouse. **P–R** Double staining for $P2X_3$-IR and IB_4 in NG of adult mouse. *Scale bar* 100 μm

cantly reduced in DRG, TG and NG. From P14 to adult mouse, $P2X_3$ receptor expression is largely restricted to a subpopulation of small-diameter neurons, with fewer large-diameter cells strongly immunopositive. The staining was evenly distributed throughout the cytoplasm of these cells and positively stained cells were apparently randomly distributed throughout the ganglia (Fig. 2).

Colocalisation of $P2X_3$ receptors with cytochemical markers of sensory neurons

In order to further identify the sensory neurons that express $P2X_3$ receptors, a number of established markers were used. In colocalisation experiments, immunolabelling for the $P2X_3$ receptor was compared with that for IB_4, CGRP, NF200 and calbindin. Briefly, as stated above, the $P2X_3$ receptor immunolabelling was evenly distributed throughout the cytoplasm of the cell body. IB_4 produced a labelled plasmalemma and diffuse speckling in the cytoplasm (Fig. 3). CGRP immunolabelling produced diffuse cytoplasmic speckling and a more diffuse perinuclear ring

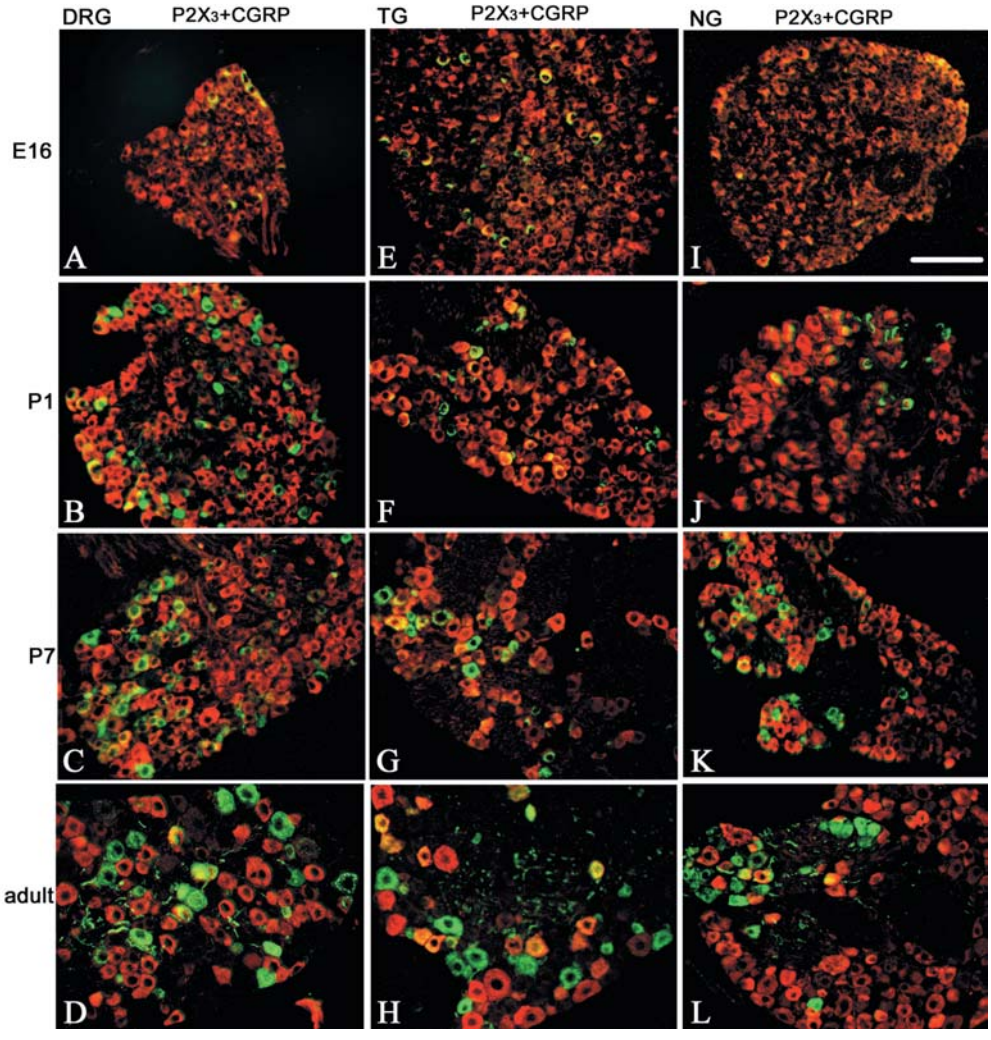

Fig. 4A–L Colocalisation (*yellow/orange*) of $P2X_3$ receptor immunoreactivity (*red*) with calcitonin gene-related peptide (*CGRP*) immunoreactivity (*green*) in the developmental mouse sensory ganglia. **A–D** Double staining for $P2X_3$-IR and CGRP-IR in DRG of mouse embryonic and postnatal development (**A** E16; **B** P1; **C** P7; **D** adult). **E–H** Double staining for $P2X_3$-IR and CGRP-IR in TG of mouse embryonic and postnatal development (**E** E16; **F** P1; **G** P7; **H** adult). **I–L** Double staining for $P2X_3$-IR and CGRP-IR in NG of mouse embryonic and postnatal development (**I** E16; **J** P1; **K** P7; **L** adult). *Scale bar* 100 μm

(Fig. 4). NF200 labelling was evenly distributed throughout the cytoplasm of the cell body, but found mainly in large neurons (Fig. 5). Calbindin labelling was seen throughout the whole cell (Fig. 6).

$P2X_3$/IB_4

The population of small [predominantly anti-neurofilament H (RT-97)-negative] DRG neurons can be subdivided into two populations, one which binds IB_4 and another which contains the neuropeptide CGRP (Silverman and Kruger 1990; Alvarez et al. 1991). These are important markers because several lines of evidence suggest that they identify subpopulations of putative nociceptors in DRG.

Isolectin B_4 was used as a marker for fluoride-resistant acid phosphatase (FRAP)-containing neurons. IB_4 labelling was observed in 56.7%, 38.3% and 49.2% of all examined adult mouse DRG, TG and NG neurons, respectively. IB_4 labelling in DRG, TG and NG of embryos was not detected until postnatal stages and was restricted to the small cell population. In P7 mouse, the number of sensory neurons binding IB_4 was increased significantly and reached adult levels at P14 (Table 2). All IB_4-positive neurons showed colocalisation with the $P2X_3$ receptor in DRG, TG and NG of P7 mice. However, the number of neurons expressing the $P2X_3$ receptor was greater than the number of IB_4-positive neurons; only 43.2%, 29.6% and 21.5% of $P2X_3$ receptor-positive neurons were also positive for IB_4 in DRG, TG and NG of P7 mice, respectively. However, from P14 there was a significant increase of 99.2%, 70.3% and 60.3% of $P2X_3$ neurons containing IB_4 in DRG, TG and NG, respectively (Table 3; Fig. 3).

$P2X_3$/CGRP

Calcitonin gene-related peptide immunoreactivity was low in DRG, TG and NG of mouse embryos, but the percentage of DRG and TG neurons expressing the peptide significantly increased from E18 (8.5%, 7.9%) to P1 (21.1%, 18.3%) and continued increasing until 2 weeks after birth, P14. The proportion of CGRP-immunoreactive neurons stabilised after the second postnatal week, but

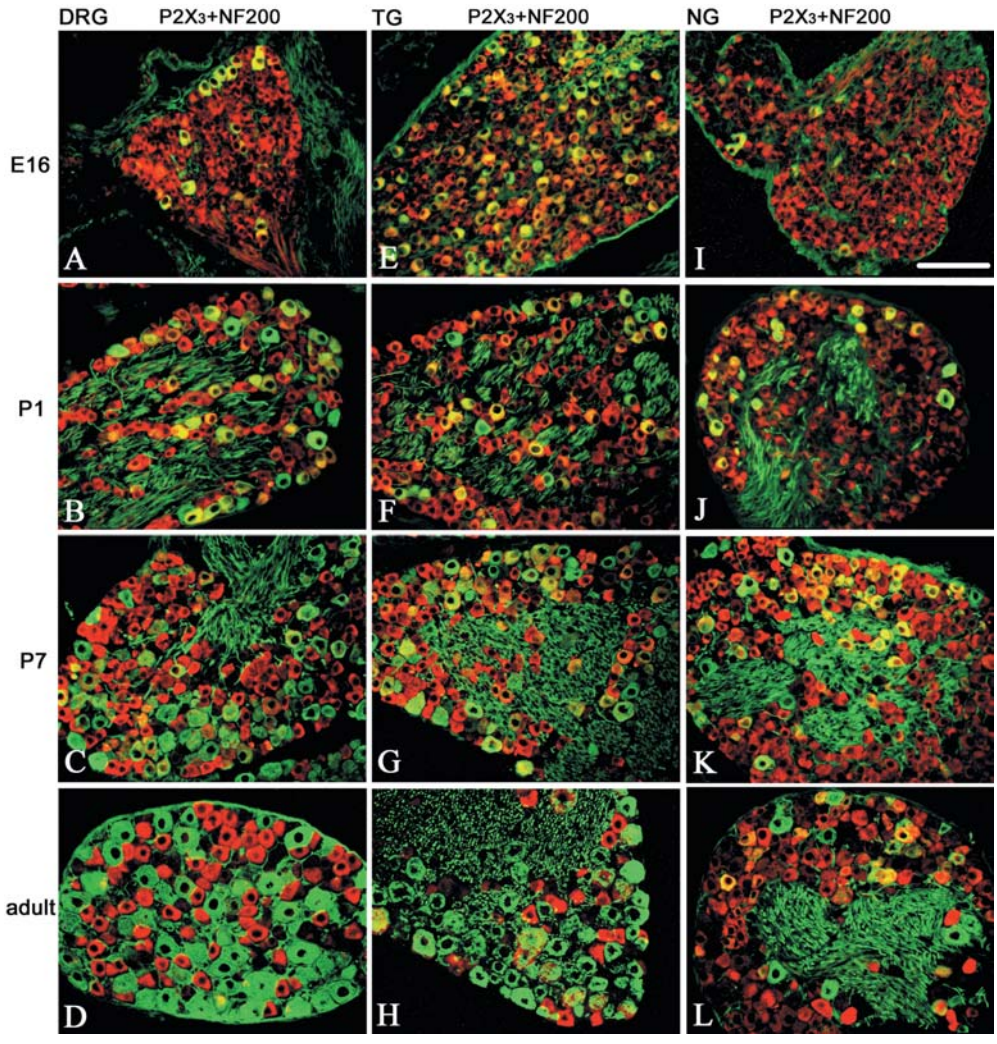

Fig. 5A–L Colocalisation (*yellow/orange*) of $P2X_3$ receptor immunoreactivity (*red*) with neurofilament 200 (*NF200*) immunoreactivity (*green*) in the developmental mouse sensory ganglia. **A–D** Double staining for $P2X_3$-IR and NF200-IR in DRG of mouse embryonic and postnatal development (**A** E16; **B** P1; **C** P7; **D** adult). **E–H** Double staining for $P2X_3$-IR and NF200-IR in TG of mouse embryonic and postnatal development (**E** E16; **F** P1; **G** P7; **H** adult). **I–L** Double staining for $P2X_3$-IR and NF200-IR in NG of mouse embryonic and postnatal development (**I** E16; **J** P1; **K** P7; **L** adult). *Scale bar* 100 μm

adult values were not statistically different from P14. In NG, CGRP immunoreactivity gradually increased after birth and reached adult levels at P14 (Table 2). Double immunofluorescence revealed that almost all neurons that were positive for CGRP (90–100%) also showed colocalisation with $P2X_3$ receptors in DRG, TG and NG of mouse embryos (Fig. 4). However, in adult mouse, only 18–34% of CGRP neuron profiles were also positive for the $P2X_3$ receptor in DRG, TG and NG. Conversely, 17.6%, 31.9% and 4.3% of $P2X_3$ receptor neurons coexpressed CGRP in DRG, TG and NG, respectively (Table 4; Fig. 4).

$P2X_3$/NF200

Neurofilament 200 is an anti-neurofilament antibody that stains the classically defined large neurons. In DRG and NG of embryos, approximately 3–15% neurons were NF200-immunoreactive positive cells. After birth, NF200 immunoreactivity was significantly increased and reached adult levels at P14 and this percentage did not significantly change in postnatal and adult mice (Table 2). Unlike DRG and NG, almost half of the neurons were NF200 immunoreactive in TG of embryos. Double immunofluorescence histochemistry showed that all NF200-immunoreactive neurons were also positive for $P2X_3$ in DRG, TG and NG in E16. However, in adult mouse, only 0.5%, 15.2%, and 49.8% of NF200-immunoreactive neuron profiles were also positive for $P2X_3$ in DRG, TG and NG, respectively (Table 5; Fig. 5).

$P2X_3$/calbindin

Calbindin-positive immunostaining was found in 5–16% of neurons in DRG, TG and NG of mouse embryos (E16). It significantly increased at postnatal P14 and remained the same in adults (Table 2). These neurons were large- or medium-sized in the DRG, TG and NG of developing mouse. Almost all calbindin-positive neurons were colocalised with $P2X_3$ receptors in DRG, TG and NG of mouse embryos. However, in adult mouse only 0.6% and 11.1% of calbindin-positive neurons were also positive for the $P2X_3$ receptor in DRG and TG, respectively. However, in NG, the number of neurons coexpressing

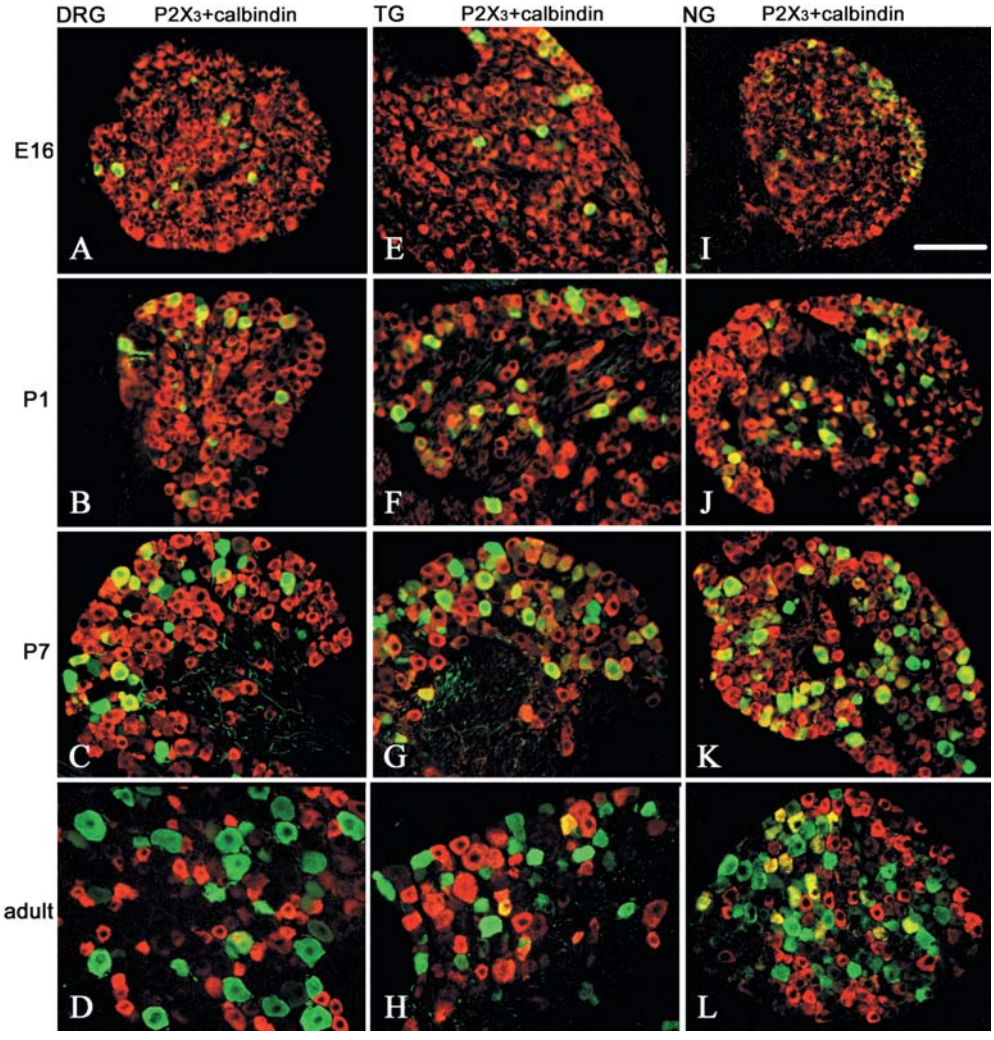

Fig. 6A–L Colocalisation (*yellow/orange*) of $P2X_3$ receptor immunoreactivity (*red*) with calbindin immunoreactivity (*green*) in the developmental mouse sensory ganglia. **A–D** Double staining for $P2X_3$-IR and calbindin-IR in DRG of mouse embryonic and postnatal development (**A** E16; **B** P1; **C** P7; **D** adult). **E–H** Double staining for $P2X_3$-IR and calbindin-IR in TG of mouse embryonic and postnatal development (**E** E16; **F** P1; **G** P7; **H** adult). **I–L** Double staining for $P2X_3$-IR and calbindin-IR in NG of mouse embryonic and postnatal development (**I** E16; **J** P1; **K** P7; **L** adult). *Scale bar* 100 μm

$P2X_3$ and calbindin (31.1%) was greater than that in DRG and TG (Table 6; Fig. 6).

Discussion

P2X receptors are ligand-gated ion channels activated by extracellular ATP that mediate rapid cation permeability and fast excitatory neurotransmission in both the central and peripheral nervous systems (reviewed by Ralevic and Burnstock 1998). One of the P2X receptor subunits, $P2X_3$, was cloned from rat dorsal root ganglia (Chen et al. 1995; Lewis et al. 1995) and is known to be largely restricted to a subset of sensory neurons (TG, NG and DRG). In this study, we present the detailed expression changes of the $P2X_3$ receptor at different stages of rat embryonic and postnatal development. In addition, the coexpression of the $P2X_3$ receptor and other phenotypic markers was also examined during embryonic and postnatal development. The results obtained have shown that the $P2X_3$ receptor is the dominant receptor subtype among the P2X receptor family in the embryonic sensory ganglion and that $P2X_3$ receptor expression is downregulated in the postnatal sensory ganglion of mouse.

In this study, we observed that the $P2X_3$ receptor is intensively and homogeneously expressed in the DRG, TG and NG from E14 to P1. However, after birth there was a gradual decline to about 50% of sensory neurons that were positive for $P2X_3$ at P14 with little further change in adults. From E14 to P7 there were mostly only small neurons, while from P7 onwards both large and small neurons were present. At P7 to adult, some large neurons stained for $P2X_3$ in TG and NG, but in DRG, for the most part, only small neurons were $P2X_3$ positive, which corresponds to the finding that approximately 40% of the DRG neurons express $P2X_3$ mRNA (Chen et al. 1995). The $P2X_3$ receptor has been demonstrated on small- or medium-sized neurons in the sensory ganglia in rat and monkey (Cook et al. 1997; Vulchanova et al. 1997; Xiang et al. 1998). The expression of $P2X_3$ receptor subunits in sensory ganglia may be involved in signal transduction and modulation as well as in regulating cellular maturation during development.

In the present work, we identified the particular class of sensory neuron that expresses $P2X_3$ receptors with the

Table 2 Changes of isolectin B_4 (IB_4), medium molecular weight neurofilament (NF200), calcitonin gene-related peptide (CGRP) and calbindin immunoreactivity in mouse embryonic and postnatal development. – Not detected, *n* number of IB_4-, NF200-, CGRP- or calbindin-positive cell profiles and the total number of cell profiles counted, respectively (five animals/stage). Note statistical significance indicated by *asterisks* relates to comparison of a developmental stage with the preceding age group

	Ganglion	E16	E18	P1	P7	P14	Adult
Percentage of IB_4 immunopositive nerve cell bodies	DRG	–	–	1.6±0.5	31.6±3.2***	49.8±2.4***	56.7±4.6
	n	(0/2,003)	(0/2,019)	(31/1,934)	(591/1,875)	(890/1,793)	(1,033/1,827)
	TG	–	–	0.8±0.2*	20.3±2.1***	35.7±3.3***	38.3±2.2
	n	(0/2,346)	(0/2,295)	(17/2,217)	(401/1,977)	(681/1,912)	(704/1,834)
	NG	–	–	0.6±0.2	18.9±2.8***	44.8±2.5***	49.2±3.4
	n	(0/1,903)	(0/1,887)	(11/1,798)	(347/1,851)	(793/1,769)	(878/1,785)
Percentage of CGRP immunopositive nerve cell bodies	DRG	6.4±1.1	8.5±0.7	21.1±3.1*	29.2±3.4	40.3±4.1	42.1±3.1
	n	(134/2,088)	(171/2,033)	(412/1,941)	(522/1,787)	(737/1,830)	(735/1,744)
	TG	5.6±0.8	7.9±0.6	18.3±1.9	33.2±3.1**	39.5±3.9	41.8±3.6
	n	(127/2,251)	(175/2,213)	(380/2,074)	(634/1,905)	(749/1,899)	(738/1,767)
	NG	1.2±0.3	2.2±0.4	5.6±0.7	10.5±1.6	13.2±1.9	15.3±2.1
	n	(25/1,962)	(41/1,835)	(102/1,813)	(185/1,774)	(228/1,742)	(272/1,787)
Percentage of NF200 immunopositive nerve cell bodies	DRG	12.8±1.5	14.6±3.3	30.5±3.1*	34.5±3.3	46.6±4.3	48.9±3.6
	n	(271/2,131)	(281/1,939)	(575/1,890)	(627/1,823)	(830/1,781)	(863/1,765)
	TG	49.6±3.6	47.5±3.9	31.6±2.8	33.7±3.5	44.8±3.5	47.7±4.4
	n	(998/2,015)	(1,006/2,124)	(688/2,175)	(653/1,943)	(896/2,002)	(856/1,794)
	NG	3.3±0.4	6.6±1.2	12.3±2.3	17.1±1.7	29.5±3.8*	32.3±3.5
	n	(65/1,944)	(126/1,927)	(230/1,884)	(307/1,792)	(508/1,721)	(582/1,805)
Percentage of calbindin immunopositive nerve cell bodies	DRG	9.6±0.9	11.8±1.4	13.5±0.9	15.6±2.2	31.8±3.7**	34.9±4.0
	n	(192/1,994)	(250/2,135)	(255/1,881)	(292/1,878)	(543/1,710)	(594/1,705)
	TG	5.2±0.4	8.8±0.8	11.7±1.7	20.4±3.5	29.7±3.2	32.8±3.7
	n	(114/2,183)	(185/2,097)	(232/1,976)	(385/1,887)	(566/1,905)	(593/1,811)
	NG	11.8±1.2	15.6±2.4	21.1±2.1	26.4±2.3	35.8±2.8	38.7±3.1
	n	(232/1,958)	(300/1,932)	(376/1,785)	(476/1,809)	(641/1,789)	(670/1,733)

* $P<0.05$
** $P<0.01$
*** $P<0.001$

Table 3 Colocalisation of $P2X_3$ receptor immunoreactivity with IB_4 in the developing mouse sensory neurons. *n* Number of double-labelled cell profiles and the total number of cell profiles counted, respectively, for each combination of receptor (five animals/stage). Note statistical significance indicated by *asterisks* relates to comparison of a developmental stage with the preceding age group

	Percentage $P2X_3$ nerve cell bodies containing IB_4			Percentage IB_4 nerve cell bodies containing $P2X_3$ receptor		
	DRG	TG	NG	DRG	TG	NG
P7	43.2±3.7	29.6±3.4	21.5±2.3	100	100	100
n	(576/1,336)	(404/1,363)	(343/1,597)	(576/576)	(404/404)	(343/343)
P14	99.2±0.4***	70.3±5.6***	60.3±4.8***	94.6±2.0	90.3±2.5	88.2±3.2
n	(880/887)	(627/891)	(652/1,081)	(880/929)	(627/694)	(652/739)
Adult	98.1±0.3	74.4±4.9	59.8±3.9	76.6±3.4***	88.5±4.6	70.6±4.4**
n	(903/921)	(631/849)	(711/1,189)	(903/1,178)	(631/713)	(711/1,007)

** $P<0.01$
*** $P<0.001$

use of double immunofluorescence immunohistochemistry. In the sensory ganglia, about 60% of the total neurons are the classically defined small population. These cells predominantly have unmyelinated C-fibre axons. Electrophysiological studies have shown that most of these cells (approximately 90%) in mouse, rat, monkey and human are nociceptive in function (Snider and McMahon 1998). These small cells can be further subdivided into two major classes according to their neurochemical phenotype (Snider and McMahon 1998): peptidergic and non-peptidergic neurons. The former, about one-half, express two major peptidergic neuromodulators, substance P and CGRP, and also the p75 neurotrophin receptor and TrkA, the NGF-specific tyrosine kinase receptor. The central terminals of these neurons project to lamina I/IIo of the superficial dorsal horn of the spinal cord, a region where many small afferents terminate. Few cells here were found to coexpress CGRP and the $P2X_3$ receptor. CGRP is the most prevalent neuropeptide identified in subpopulations of primary afferent neurons, constituting 40–50% of DRG and TG neurons (Lee et al. 1985; Ju et al. 1987; Kai-Kai 1989). The other half of the C-fibre population does not express NGF receptors (McMahon et al. 1994; Averill et al. 1995) but can be identified by a number of markers: they bind IB_4, express the enzyme thiamine monophosphatase (TMP) and stain with the antibody LA4 (marker of a population of primary afferents in the dorsal horn). They also express the heat-responsive vanilloid receptor, VR1 (Caterina et al. 1997), which implicates them in thermal nociception. The central terminals of these neurons project to inner lamina 2 of the superficial dorsal horn of the spinal cord, another region

Table 4 Colocalisation of $P2X_3$ receptor immunoreactivity with CGRP in the developmental mouse sensory neurons. *n* Number of double-labelled cell profiles and the total number of cell profiles counted, respectively, for each combination of receptor (five animals/stage). Note statistical significance indicated by *asterisks* relates to comparison of a developmental stage with the preceding age group

	Percentage $P2X_3$ receptor-positive neurons containing CGRP			Percentage CGRP-positive neurons containing the $P2X_3$ receptor		
	DRG	TG	NG	DRG	TG	NG
E16	6.4±1.0	5.6±0.7	1.2±0.3	100	100	100
n	(141/2,203)	(135/2,411)	(27/2,178)	(141/141)	(135/135)	(27/27)
E18	7.8±1.7	7.6±0.5	2.2±0.8	90.2±1.7*	92.3±2.5	93.6±1.8
n	156/2,010	(161/2,118)	(39/1,772)	(156/173)	(161/175)	(39/42)
P1	9.3±1.9	11.8±1.6	3.2±1.0	38.7±3.1***	56.6±3.9***	45.6±3.6***
n	(170/1,825)	(233/1,976)	(58/1,807)	(170/439)	(233/412)	(58/127)
P7	14.3±1.5	19.5±2.3	5.4±0.7	35.5±2.5	40.4±3.7*	34.4±2.9*
n	(202/1,413)	(251/1,289)	(81/1,502)	(202/569)	(251/622)	(81/235)
P14	18.3±2.1	29.8±3.0*	4.9±0.7	21.6±1.7**	35.6±3.3	21.2±2.3**
n	(168/921)	(258/868)	(51/1,038)	(168/778)	(258/725)	(51/241)
Adult	17.6±2.7	31.9±2.9	4.3±0.8	18.5±2.3	33.4±4.1	18.1±1.3
n	(153/872)	(273/857)	(48/1,119)	(153/827)	(273/818)	(48/266)

* $P<0.05$
** $P<0.01$
*** $P<0.001$

Table 5 Colocalisation of $P2X_3$ receptor immunoreactivity with NF200 in the developmental mouse sensory neurons. *n* Number of double-labelled cell profiles and the total number of cell profiles counted, respectively, for each combination of receptor (five animals/stage). Note statistical significance indicated by *asterisks* relates to comparison of a developmental stage with the preceding age group

	Percentage $P2X_3$ nerve cell bodies containing NF200			Percentage NF200 nerve cell bodies containing $P2X_3$ receptor		
	DRG	TG	NG	DRG	TG	NG
E16	12.8±1.3	49.6±3.3	3.3±0.3	100	100	100
n	(263/2,053)	(987/1,990)	(65/1,969)	(263/263)	(987/987)	(65/65)
E18	14.9±1.9	49.5±4.1	7.0±0.6	99.3±0.4	97.5±0.9	98.6±0.7
n	(278/1,866)	(991/2,001)	(123/1,756)	(278/280)	(991/1,016)	(123/125)
P1	23.3±2.7**	24.8±2.3**	11.5±1.9	70.8±6.5***	72.5±4.1***	90.1±1.1
n	(487/2,090)	(541/2,181)	(209/1,816)	(487/688)	(541/747)	(209/232)
P7	8.5±07**	23.2±2.3	24.8±2.0**	17.7±1.5***	46.6±3.8***	87.9±4.5
n	(117/1,386)	303/1,309	(350/1,413)	(117/662)	(303/651)	(350/398)
P14	2.0±0.4	17.9±2.8	23.5±3.1	2.1±0.4**	18.3±2.1***	52.3±4.9***
n	(18/886)	(158/883)	(271/1,154)	(18/857)	(158/864)	(271/518)
Adult	0.6±0.3	17.5±2.3	26.5±2.6	0.5±0.2	15.2±1.8	49.8±3.8
n	(5/857)	(145/831)	(288/1,086)	(5/943)	(145/953)	(288/578)

** $P<0.01$
*** $P<0.001$

Table 6 Colocalisation of $P2X_3$ receptor immunoreactivity with calbindin in the developmental mouse sensory neurons. *n* Number of double-labelled cell profiles and the total number of cell profiles counted, respectively, for each combination of receptor (five animals/stage). Note statistical significance indicated by *asterisks* relates to comparison of a developmental stage with the preceding age group

	Percentage $P2X_3$ receptor nerve cell bodies containing calbindin			Percentage calbindin nerve cell bodies containing $P2X_3$ receptor		
	DRG	TG	NG	DRG	TG	NG
E16	9.6±0.8	5.2±0.4	11.8±1.1	100	100	100
n	(204/2,125)	(121/2,336)	(239/2,031)	(204/204)	(121/121)	(239/239)
E18	12.1±1.4	9.2±0.8	15.9±1.9	100	100	100
n	(241/1,989)	(189/2,059)	(286/1,801)	(241/241)	(189/189)	(286/286)
P1	14.3±1.7	12.4±1.3	20.3±1.6	98.2±0.8	97.5±1.2	92.7±3.5
n	(257/1,793)	(237/1,915)	(362/1,784)	(257/262)	(237/243)	(362/391)
P7	8.8±1.8	17.5±1.9	21.1±2.2	46.8±3.1***	58.9±5.4***	70.3±6.7**
n	(123/1,392)	(232/1,322)	(341/1,618)	(123/263)	(232/394)	(341/485)
P14	3.2±0.9*	9.2±1.5**	18.8±1.7	5.1±0.6***	13.6±1.8***	34.5±3.2***
n	(29/903)	(79/859)	(215/1,147)	(29/569)	(79/581)	(215/623)
Adult	0.4±0.2	8.3±1.1	19.8±2.1	0.6±0.2	11.1±2.1	31.1±2.4
n	(3/789)	(68/817)	(198/997)	(3/523)	(68/612)	(198/637)

* $P<0.05$
** $P<0.01$
*** $P<0.001$

where many fine afferents terminate. In vivo studies (Gerke and Plenderleith 2001) demonstrate that IB_4-binding sites are selectively expressed by nociceptive afferents. Physiological studies demonstrate that some IB_4-binding DRG neurons are deep tissue, high-threshold mechanoreceptors and polymodal nociceptors. In our experiments, we found that IB_4-positive neurons in DRG, TG and NG did not appear until birth, but the numbers increased to about 50% by P14 with little further change in adults. We also found that about 10% of neurons in DRG, TG and NG were positive for CGRP in embryos, but this increased postnatally to about 35–40% in adults, except for NG where CGRP immunoreactivity only reached about 15% in adults.

To characterise the cytochemical profile of $P2X_3$-positive neurons, we examined the colocalisation of the $P2X_3$ receptor with IB_4 and CGRP. At P7, a few $P2X_3$-positive neurons in DRG,TG and NG stained for IB_4, but by P14 and in adults a high proportion of IB_4-positive neurons also labelled $P2X_3$. In contrast, in the embryo nearly 100% of CGRP-positive neurons, albeit relatively few, stained for $P2X_3$, but by postnatal P14 and in adult ganglia only about 20% in DRG and NG and 35% in TG showed colocalisation of CGRP and $P2X_3$ receptors. Since IB_4 has been shown to label almost all FRAP-positive neurons (Wang et al. 1994), and because we found little colocalisation of the $P2X_3$ receptor with CGRP in adults, our results indicate that $P2X_3$ is predominantly expressed by FRAP-containing DRG and TG neurons. This conclusion is supported by the extensive colocalisation of $P2X_3$ and LA4-IR; LA4 also labels almost all FRAP-positive cells (Dodd and Jessell 1985). It has been proposed that FRAP-containing and peptide-containing sensory neurons represent two parallel systems for processing of nociceptive information (Hunt and Rossi 1985). A nociceptive role for FRAP-positive neurons is also suggested by the localisation of the enzyme activity in nerve fibres in cornea (Silverman and Kruger 1988) and in tooth pulp primary afferents (Fried et al. 1989), as these peripheral targets are thought to be innervated primarily by nociceptors. Unlike DRG and TG, in NG, the highest intensity of $P2X_3$ neurons was most often observed within the small IB_4-negative population. The types of overlap in the binding of IB_4 and coexpression of $P2X_3$ receptor, described in the present study for NG neurons, is both similar and different from the patterns described for DRG and TG neurons. A continued focus using these and other population markers for each of these functionally different neuronal populations (i.e. NG versus DRG, TG) has the potential for identifying a unique neuronal fingerprint for the processing of visceral sensory information.

The large cells within the sensory neurons are rich in neurofilament. We identified these cells with the antibody NF200 and found that NF200 was expressed in about 50% of neurons in TG in the embryo, which persisted in postnatal and adult mice. However, a relatively low percentage of NF200-positive neurons were present in embryonic DRG and NG, but the percentage increased substantially by P14 and in adults, when many of the neurons became large, especially in NG. In the embryo, all NF200-positive neurons stained for $P2X_3$ in DRG, TG and NG, but by adulthood this was reduced to 0.5%, 15% and 50% in these ganglia, respectively. The $P2X_3$ receptor was expressed not only in small- and medium-sized neurons, but also in large neurons of TG and NG. The large neurofilament-rich neurons are known to possess myelinated axons and to be predominantly responsive to non-nociceptive innocuous mechanical stimuli.

Calbindin-D28 k is widely represented in the nervous system and is used as a cellular marker for neuroanatomical studies along with other calcium-binding proteins such as parvalbumin and calretinin (Andressen et al. 1993). Calbindin-D28 k immunoreactivity has been observed in the sensory and autonomic ganglia such as the DRG, TG, jugular ganglion and superior cervical ganglion (Carr et al. 1989; Ichikawa and Helke 1995; Ichikawa et al. 1996; Wakisaka et al. 1996; Grkovic and Anderson 1997). In the present study, we observed calbindin-positive immunostaining in 5–12% of neurons in DRG, TG and NG of mouse embryos. Expression is increased gradually postnatally and reached adult levels at P14. Almost all calbindin-positive neurons were colocalised with $P2X_3$ receptors in DRG, TG and NG of mouse embryos. In contrast, in adult DRG and TG, few showed colocalisation, 0.6% and 11%, respectively (because calbindin is mostly present in large neurons), while in adult NG, where there are many large neurons, 31% showed colocalisation. These results are consistent with those previously reported (Kashiba et al. 1990; Honda 1995; Ichikawa and Helke 1995; Ichikawa et al. 1996). These findings suggest that the $P2X_3$ receptor is related to cutaneous sensory neurons in DRG and TG and splanchnic sensory neurons in NG.

References

Alavi AM, Dubyak GR, Burnstock G (2001) Immunohistochemical evidence for ATP receptors in human dental pulp. J Dental Res 80:476–483

Alvarez FJ, Morris HR, Priestely JC (1991) Sub-populations of smaller diameter trigeminal primary afferent neurons defined by expression of calcitonin gene-related peptide and the cell surface oligosaccharide recognized by monoclonal antibody LA4. J Neurocytol 20:716–731

Andressen C, Blumcke I, Celio MR (1993) Calcium-binding proteins: selective markers of nerve cells. Cell Tissue Res 271:181–208

Averill S, McMahon SB, Clary DO, Reichardt LF, Priestley JV (1995) Immunocytochemical localization of trkA receptors in chemically identified subgroups of adult rat sensory neurons. Eur J Neurosci 7:1484–1494

Barden JA, Bennett MR (2000) Distribution of P2X purinoceptor clusters on individual rat dorsal root ganglion cells. Neurosci Lett 287:183–186

Bo X, Alavi A, Xiang Z, Oglesby I, Ford A, Burnstock G (1999) Localization of ATP-gated $P2X_2$ and $P2X_3$ receptor immunoreactive nerves in rat taste buds. Neuroreport 10:1107–1111

Boldogkö IZ, Schütz B, Sallach J, Zimmer A (2002) $P2X_3$ receptor expression at early stage of mouse embryogenesis. Mech Dev 118:255–260

Bradbury EJ, Burnstock G, McMahon SB (1998) The expression of $P2X_3$ purinoceptors in sensory neurons: effects of axotomy and glial-derived neurotrophic factor. Mol Cell Neurosci 12:256–268

Burnstock G (1996) Purinoceptors: ontogeny and phylogeny. Drug Dev Res 39:204–242

Burnstock G (2001) Purinergic signalling in development. In: Abbracchio MP, Williams M (eds) Handbook of experimental pharmacology, vol 151/I. Purinergic and pyrimidinergic signalling. I. Molecular, nervous and urogenitary system function. Springer, Berlin Heidelberg New York, pp 89–127

Carr PA, Yamamoto T, Karmy G, Baimbridge KG, Nagy JI (1989) Parvalbumin is highly colocalized with calbindin D28 k and rarely with calcitonin gene-related peptide in dorsal root ganglia neurons of rat. Brain Res 497:163–170

Caterina MJ, Schumacher MA, Tominage M, Rosen TA, Levine JD, Julius D (1997) The capsaicin receptor: a heat-activated ion channel in the pain pathway. Nature 389:816–824

Chen CC, Akopian AN, Sivilotti L, Colquhoun D, Burnstock G, Wood JN (1995) A P2X receptor expressed by a subset of sensory neurons. Nature 377:428–430

Cheung K, Burnstock G (2002) Localization of $P2X_3$ receptors and coexpression with $P2X_2$ receptors during rat embryonic neurogenesis. J Comp Neurol 443:368–382

Cockayne DA, Hamilton SG, Zhu Q-M, Dunn PM, Zhong Y, Novakovic S, Malmberg AB, Cain G, Berson A, Kassotakis L, Lachnit WG, Burnstock G, McMahon SB, Ford APDW (2000) Urinary bladder hyporeflexia and reduced pain-related behaviour in $P2X_3$-deficient mice. Nature 407:1011–1015

Cook SP, Vulchanova L, Hargreaves KM, Elde R, McCleskey EW (1997) Distinct ATP receptors on pain-sensing and stretch-sensing neurons. Nature 387:505–508

Dodd J, Jessell TM (1985) Lactoseries carbohydrates specify subsets of dorsal root ganglion neurons projecting to the superficial dorsal horn of rat spinal cord. J Neurosci 5:3278–3294

Dunn PM, Liu M, Zhong Y, King BF, Burnstock G (2000) Diinosine pentaphosphate: an antagonist which discriminates between recombinant P2X(3) and P2X(2/3) receptors and between two P2X receptors in rat sensory neurons. Br J Pharmacol 130:1378–1384

Dunn PM, Zhong Y, Burnstock G (2001) P2X receptors in peripheral neurons. Prog Neurobiol 65:107–134

Fried K, Arvidsson J, Robertson B, Brodin E, Theodorsson E (1989) Combined retrograde tracing and enzyme/immunohistochemistry of trigeminal ganglion cell bodies innervating tooth pulps in the rat. Neuroscience 33:101–109

Gerke MB, Plenderleith MB (2001) Binding sites for the plant lectin *Bandeiraea simplicifolia* I-isolectin B(4) are expressed by nociceptive primary sensory neurons. Brain Res 911:101–104

Grkovic I, Anderson CR (1997) Calbindin D28k-immunoreactivity identifies distinct subpopulations of sympathetic pre- and postganglionic neurons in the rat. J Comp Neurol 386:245–259

Guo A, Vulchanova L, Wang J, Li X, Elde R (1999) Immunocytochemical localization of the vanilloid receptor 1 (VR1): relationship to neuropeptides, the $P2X_3$ purinoceptor and IB_4 binding sites. Eur J Neurosci 11:946–958

Honda CN (1995) Differential distribution of calbindin-D28 k and parvalbumin in somatic and visceral sensory neurons. Neuroscience 68:883–892

Hunt SP, Rossi J (1985) Peptide and non peptide containing unmyelinated primary afferents: the parallel processing of nociceptive information. Philos Trans R Soc Lond B 308:283–289

Ichikawa H, Helke CJ (1995) Parvalbumin and calbindin D-28 k in vagal and glossopharyngeal sensory neurons of the rat. Brain Res 675:337–341

Ichikawa H, Deguchi T, Fujiyoshi Y, Nakago T, Jacobowitz DM, Sugimoto T (1996) Calbindin-D28k-immunoreactivity in the trigeminal ganglion neurons and molar tooth pulp of the rat. Brain Res 715:71–78

Ju G, Hökfelt T, Brodin E, Fahrenkrug J, Fischer JA, Frey P, Elde RP, Brown JC (1987) Primary sensory neurons of the rat showing calcitonin gene-related peptide immunoreactivity and their relation to substance P-, somatostatin-, galanin-, vasoactive intestinal polypeptide- and cholecystokinin-immunoreactive ganglion cells. Cell Tissue Res 247:417–431

Kai-Kai MA (1989) Cytochemistry of the trigeminal and dorsal root ganglia and spinal cord of the rat. Comp Biochem Physiol 93A:183–193

Kashiba H, Senba E, Ueda Y, Tohyama M (1990) Calbindin D28k-containing splanchnic and cutaneous dorsal root ganglion neurons of the rat. Brain Res 528:311–316

Laasberg T (1990) Ca^{2+}-mobilizing receptors of gastrulating chick embryo. Comp Biochem Physiol C97:1–12

Lee Y, Kawai Y, Shiosaka S, Takami K, Kiyama H, Hillyard CJ, Girgis S, MacIntyre I, Emson PC, Tohyama M (1985) Coexistence of calcitonin gene-related peptide and substance P-like peptide in single cells of the trigeminal ganglion of the rat: immunocytochemical analysis. Brain Res 330:194–196

Lewis C, Neidhart S, Holy C, North RA, Buell G, Suprenant A (1995) Coexpression of $P2X_2$ and $P2X_3$ receptor subunits can account for ATP-gated currents in sensory neurons. Nature 377:432–434

Liu M, King BF, Dunn PM, Rong W, Townsend-Nicholson A, Burnstock G (2001) Coexpression of P2X(3) and P2X(2) receptor subunits in varying amounts generates heterogeneous populations of P2X receptors that evoke a spectrum of agonist responses comparable to that seen in sensory neurons. J Pharmacol Exp Ther 296:1043–1050

Llewellyn-Smith IJ, Burnstock G (1998) Ultrastructural localization of $P2X_3$ receptors in rat sensory neurons. Neuroreport 9:2245–2250

McMahon SB, Armanini MP, Ling LH, Phillips HS (1994) Expression and coexpression of Trk receptors in subpopulations of adult primary sensory neurons projecting to identified peripheral targets. Neuron 12:1161–1171

Novakovic SD, Kassotakis LC, Oglesby IB, Smith JAM, Eglen RM, Ford APDW, Hunter JC (1999) Immunocytochemical localization of $P2X_3$ purinoceptors in sensory neurons in naive rats and following neuropathic injury. Pain 80:273–282

Ralevic V, Burnstock G (1998) Receptors for purines and pyrimidines. Pharmacol Rev 50:413–492

Rong W, Burnstock G, Spyer KM (2000) P2X purinoceptor-mediated excitation of trigeminal lingual nerve terminals in an in vitro intra-arterially perfused rat tongue preparation. J Physiol 524:891–902

Rong W, Spyer KM, Burnstock G (2002) Activation and sensitisation of low and high threshold afferent fibres mediated by P2X receptors in the mouse urinary bladder. J Physiol 541:591–600

Silverman JD, Kruger L (1988) Lectin and neuropeptide labeling of separate populations of dorsal rat testis and cornea whole mount preparations. Somatosens Res 5:259–267

Silverman JD, Kruger L (1990) Selective neuronal glycoconjugate expression in sensory and autonomic ganglia: relation of lectin reactivity to peptide and enzyme markers. J Neurocytol 19:789–801

Snider WD, McMahon SB (1998) Tackling pain at the source: new insights into nociceptors. Neuron 20:629–632

Souslova V, Cesare P, Ding Y, Akopian AN, Stanfa L, Suzuki R, Carpenter K, Dickenson A, Boyce S, Hill R, Nebenuis-Oosthuizen D, Smith AJ, Kidd EJ, Wood JN (2000) Warm-coding deficits and aberrant inflammatory pain in mice lacking $P2X_3$ receptors. Nature 407:1015–1017

Ueno S, Tsuda M, Iwanaga T, Inoue K (1999) Cell type-specific ATP-activated responses in rat dorsal root ganglion neurons. Br J Pharmacol 126:429–436

Vlaskovska M, Kasakov L, Rong W, Bodin P, Bardini M, Cockayne DA, Ford AP, Burnstock G (2001) $P2X_3$ knock-out mice reveal a major sensory role for urothelially released ATP. J Neurosci 21:5670–5677

Vulchanova L, Arvidsson U, Riedl M, Wang J, Buell G., Surprenant A, North RA, Elde R (1997) Immunocytochemical study of the $P2X_2$ and $P2X_3$ receptor subunits in rat and

monkey sensory neurons and their central terminals. Neuropharmacology 36:1229–1242

Vulchanova L, Riedl MS, Shuster SJ, Stone LS, Hargreaves KM, Buell G., Surprenant, A, North RA, Elde R (1998) $P2X_3$ is expressed by DRG neurons that terminate in inner lamina II. Eur J Neurosci 10:3470–3478

Wakisaka S, Takikita S, Youn SH, Kurisu K (1996) Partial coexistence of neuropeptide Y and calbindin D28 k in the trigeminal ganglion following peripheral axotomy of the inferior alveolar nerve in the rat. Brain Res 707:228–234

Wang H, Rivero Melian C, Robertson B, Grant G (1994) Transganglionic transport and binding of the isolectin B4 from *Griffonia simplicifolia* I in rat primary sensory neurons. Neuroscience 62:539–551

Xiang Z, Bo X, Burnstock G (1998) Localization of ATP-gated P2X receptor immunoreactivity in rat sensory and sympathetic ganglia. Neurosci Lett 256:105–108

Zhong Y, Dunn PM, Bardini M, Ford AP, Cockayne DA, Burnstock G (2001) Changes in P2X receptor responses of sensory neurons from $P2X_3$-deficient mice. Eur J Neurosci 14:1784–1792